International Journal of Electrical, Electronic and Communication Sciences
ISSN: 2517-9438
Vol:6, No:1, 2012

Observers Design for Systems Modelled by Bond Graphs with Multivariable Monotone Nonlinearities

Gilberto Gonzalez-A, Gerardo Jaimes-A

***Abstract*—**A methodology to design a nonlinear observer in a bond graph approach is proposed. The class of nonlinear observer with multivariable nonlinearities is considered. A junction structure of the bond graph observer is proposed. The proposed methodology to an electrical transformer and a DC motor including the nonlinear saturation is applied. Nonlinear observers for the transformer and DC motor based on multivariable circle criterion in the physical domain are proposed. In order to show the saturation effects on the transformer and DC motor, simulation results are obtained. Finally, the paper describes that convergence of the estimates to the true states is achieved.

***Keywords*—**Bond graph, nonlinear observer, electrical transformer, nonlinear saturation

I. Introduction

BOND graph methodology provides a formal and systematic language for modeling dynamic systems. It incorporates physical assumptions and issues made about system models in an explicit and precise way. In practical engineering, bond graphs are typically used to help generate the differential or the state equations of systems for standard numerical simulation. However, they can also be used for various forms of qualitative reasoning which made no reference to system differential equations at all.

Hence, the bond graph approach has been developed in recent years as a powerful tool for modeling dynamical systems. It essentially focusses on the exchange of energy between the system and its enviroment and between different elements within the system. It is this energy exchange that determines the dynamics of any system.

The bond graph method is acknowledged to be highly suited for dynamic modeling because of the following reasons: (a) the derivation of system equations can be algorithmized; (b) nonlinear elements are easily modeled.

On the other hand, the principle of observability intuitively establishes the possibility to rebuilt the state variables from the measured outputs and given inputs. With observability conditions, the observation problem consists in seeking a state estimation by means of an auxiliary dynamic system, the observer [4].

Gilberto Gonzalez-A is with the Faculty of Electrical Engineering, University of Michoacan (e-mail: gilmichga@yahoo.com.mx)

Gerardo Jaimes-A is with Faculty of Electrical Engineering, University of Michoacan (e-mail: remegan@ieee.org).

In [14] presents a new method using bond graph methodology to derive information on structural controllability/observability properties of a system.

Also, some papers have been published applying bond graph to construct an observer. In [5] proposes a control in bond graph using state estimated feedback for MIMO LTI systems. In [6] a bond graph approach to built reduced order observers for LTI systems is described. This approach uses the bicausality concept to simplify the construction and the calculation of the observer. A bond graph representation of model-based control, which allows the design of controllers in the physical domain is described in [7].

In other wise many papers have been published on observers, for example [8] gives an approach to estimate the state of a nonlinear system from the point of view of differential algebra. However, in [9] and [10] globally convergent observers are designed for a class of systems with multivariable nonlinearities. Also, most of the existing nonlinear observer designs restrict the system to be linear in the unmeasured states.

Thus, the main contribution of this paper is to design an observer in a bond graph approach for systems with multivariable monotone nonlinearities. In this paper a bond graph model of a transformer with two windings is proposed. Also, a basic electromagnetic model for the magnetizing branch of a transformer with two windings in the physical domain is described. This magnetizing branch consists of a resistor and inductance. However, in order to introduce the magnetic saturation a nonlinear function is used.

According with transformers, in [11] a magnetic circuit model of power transformer which takes into account the nonlinear hysteresis phenomenon is analyzed. However, this paper uses a special nonlinear function to introduce the hysteresis. In [13] a bond graph model of a transformer based on a nonlinear conductive magnetic circuit is described. Here, the state space nonlinear magnetic model has to be known. Also, the nonlinear function to armature inductance of a DC motor is applied. Then, an observer for the DC motor is designed.

Section II gives some basic elements of the modeling in bond graph. Section III describes the observers design for a class of nonlinear system with multivariable nonlinearities. A nonlinear observer in the physical domain is presented in section IV. A bond graph model of a transformer with two windings considering the nonlinear core is proposed in section

V. In this section, nonlinear observer in the physical domain of the transformer is presented. Section VI, describes a bond graph of a DC motor and the bond graph observer is proposed. Finally, section VII gives the conclusions.

II. Modeling in Bond Graph

The bond graph methodology allows to model a system in a simple and direct manner. Using fields and junction structures, one may conveniently study systems containing complex multiport components using bond graphs. In fact, bond graphs with fields prove to be a most effective way to handle the modeling of complex multiport systems [2].

Consider the following scheme of a multiport LTI system which includes the key vectors of Fig. 1 [2], [14].

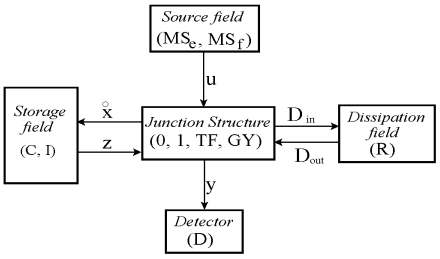

Fig. 1 Key vectors of a bond graph

In Fig. 1, (MSe, MSf), (C, I), (R) and (D) denote the source, the energy storage, the energy dissipation and the detector fields, and $(0,1,TF,GY)$ the junction structure with transformers, TF, and gyrators, GY.

The state $x \in \Re^n$ is composed of energy variables p and q associated with I and C elements in integral causality assignment, $u \in \Re^p$ denotes the plant input, $y \in \Re^q$, the plant output, $z \in \Re^n$ the co-energy vector, and $D_{in} \in \Re^r$ and $D_{out} \in \Re^r$ are a mixture of e and f showing the energy exchanges between the dissipation field and the junction structure.

The relations of the storage and dissipation field are,

$$z(t) = Fx(t) \tag{1}$$

$$D_{out}(t) = LD_{in}(t) \tag{2}$$

The relations of the junction structure are [2], [14],

$$\begin{bmatrix} \dot{x}(t) \\ D_{in}(t) \\ y(t) \end{bmatrix} = \begin{bmatrix} S_{11} & S_{12} & S_{13} \\ S_{21} & S_{22} & S_{23} \\ S_{31} & S_{32} & S_{33} \end{bmatrix} \begin{bmatrix} z(t) \\ D_{out}(t) \\ u(t) \end{bmatrix} \tag{3}$$

The entries of S take values inside the set $\{0, \pm 1, \pm K_t, \pm K_g\}$ where K_t and K_g are transformer and gyrator modules; S_{11} and S_{22} are square skew-symmetric matrices and S_{12} and S_{21} are matrices each other negative transpose. The state equation is,

$$\dot{x}(t) = A_p x(t) + B_p u(t) \tag{4}$$

$$y(t) = C_p x(t) + D_p u(t) \tag{5}$$

where

$$A_p = (S_{11} + S_{12} M S_{21}) F \tag{6}$$

$$B_p = S_{13} + S_{12} M S_{23} \tag{7}$$

$$C_p = (S_{31} + S_{32} M S_{21}) F \tag{8}$$

$$D_p = S_{33} + S_{32} M S_{23} \tag{9}$$

being

$$M = (I - LS_{22})^{-1} L \tag{10}$$

It is very common in electrical power systems to use the electrical current as state variable of this manner taking the derivative of (1) and (4), we have

$$\dot{z}(t) = \overline{A_p} z(t) + \overline{B_p} u(t) \tag{11}$$

$$y = \overline{C_p} z(t) + D_p u(t) \tag{12}$$

where

$$\overline{A_p} = F A_p F^{-1} \tag{13}$$

$$\overline{B_p} = F B_p \tag{14}$$

$$\overline{C_p} = C_p F^{-1} \tag{15}$$

Next section describes the design of an observer for systems with multivariable monotone nonlinearities.

III. A Nonlinear Observer

This design represents the observer error system as the feedback interconnection of a linear system and a state-dependent sector nonlinearity [9].

Firstly, this observer uses the multivariable nonlinearities $\gamma(\bullet): \Re^l \to \Re^l$ which satisfy a multivariable analog of the monotonicity property:

$$\frac{\partial \gamma}{\partial \upsilon} + \left(\frac{\partial \gamma}{\partial \upsilon} \right)^T \geq 0 \forall \upsilon \in \Re^l \tag{16}$$

With this property, the state nonlinearity that arises in the observer error system a multivariable sector condition. For our observer design, we consider the plant

$$\begin{aligned} \dot{x}(t) &= A_p x(t) + G\gamma(Hx(t)) + B_p u(t) \\ y(t) &= C_p x(t) \end{aligned} \tag{17}$$

where $x \in \Re^n$ is the state, $y \in \Re^q$ is the measured output, $u \in \Re^p$ is the control input, and the multivariable nonlinearity $\gamma(\bullet): \Re^l \to \Re^l$ satisfies (16).

With this assumption, our observer has the same form as in [16]:

$$\begin{aligned} \dot{\hat{x}} = {} & A_p \hat{x}(t) + L(C\hat{x}(t) - y(t)) + \\ & G\gamma(H\hat{x}(t) + K(C\hat{x}(t) - y(t))) + B_p u(t) \end{aligned} \tag{18}$$

Our task is to determine the observer matrices $K \in \Re^{l \times q}$ and $L \in \Re^{n \times q}$ to make the observer error $e(t) = x(t) - \hat{x}(t)$ approach zero. From (17) and (18), the dynamics of the observer error $e(t) = x(t) - \hat{x}(t)$ are governed by

$$\dot{e}(t) = (A_p + LC_p) e(t) + G[\gamma(\upsilon) - \gamma(\omega)] \tag{19}$$

where

$$\upsilon = Hx, \omega = H\hat{x}(t) + K(C_p \hat{x}(t) - y(t)) \tag{20}$$

We begin the observer design by representing the observer error system (19) as the feedback interconnection of a linear system and multivariable sector nonlinearity. To this end, we view $\gamma(\upsilon)-\gamma(\omega)$ as a function of υ and $z=\upsilon-\omega=(H+KC)e$; that is, a state-dependent multivariable nonlinearity in z:

$$\varphi(\upsilon,z)=\gamma(\upsilon)-\gamma(\omega) \tag{21}$$

Substituting (21), we rewrite the observer error system (19) as

$$\begin{aligned}\dot{e}(t)&=(A_p+LC_p)e(t)+G\varphi(\upsilon,z)\\ z(t)&=(H+KC_p)e(t)\end{aligned} \tag{22}$$

To show that $\varphi(\upsilon,z)$ satisfies a multivariable sector property, we make use the Mean Value Theorem [9], and rewrite $\varphi(\upsilon,z)$ as

$$\begin{aligned}\varphi(\upsilon,z)&=\gamma(\upsilon)-\gamma(\omega)\\ &=\int_0^1\left[\frac{\partial\gamma}{\partial s}\right]_{s=\upsilon+\lambda(\omega-\upsilon)}(\upsilon-\omega)\,d\lambda\\ &=\int_0^1\left[\frac{\partial\gamma}{\partial s}\right]_{s=\upsilon-\lambda z}\end{aligned} \tag{23}$$

Thus, from property (16),

$$z^T\varphi(\upsilon,z)=\frac{1}{2}\int_0^1\left(\left[\frac{\partial\gamma}{\partial s}\right]+\left[\frac{\partial\gamma}{\partial s}\right]^T\right)_{s=\upsilon-\lambda z}d\lambda z\geq 0 \tag{24}$$

Thanks to this sector property, asymptotic stability is guaranteed from the circle criterion if the linear system with input $\vartheta=-\varphi(\upsilon,z)$ and output z is SPR, that is, if a matrix $P=P^T>0$, and a constant $\varsigma>0$ can be found such that [9]

$$\begin{bmatrix}(A+LC)^TP+P(A+LC)+\varsigma I & PG+(H+KC)^T\\ G^TP+(H+KC) & 0\end{bmatrix}\leq 0 \tag{25}$$

Thus, the observer design for system (17) consists on solving (25), which is LMI in $P=P^T\geq 0$, P,L,K and $\varsigma\geq 0$.

Next section presents a general scheme to obtain an observer in the physical domain.

IV. An Observer Based on a Bond Graph

A direct graphical technique to obtain the observer of a system represented by bond graph is presented. It is important to note that the magnetizing inductance is a nonlinear function described by (41). Thus, the proposed observer is a nonlinear system. The general structure of the complete system is shown in Fig. 2.

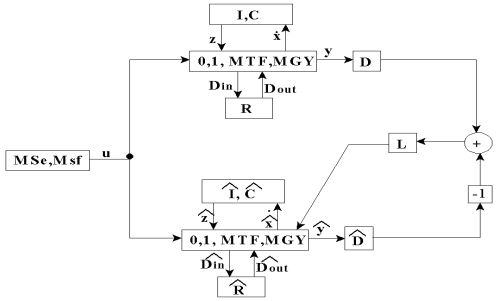

The objective to represent the model and the observer in block diagrams is to obtain the complete system in terms of the junction structure matrices. This let us to know, the change of S due to the observer with the purpose the assign the gains of the observer.

The structure of the observer is given by,

$$\begin{bmatrix}\dot{\hat{x}}(t)\\ \hat{D}_{in}(t)\\ \hat{y}(t)\end{bmatrix}=\hat{S}\begin{bmatrix}\hat{z}(t)\\ \hat{D}_{out}(t)\\ u(t)\end{bmatrix}+\tilde{S}z(t) \tag{26}$$

The state space representation of the observer is,

$$\dot{\hat{x}}=\hat{A}_p\hat{x}(t)+\hat{B}_pu(t)+\tilde{S}Fx(t) \tag{27}$$

$$\hat{y}(t)=\hat{C}_p\hat{x}(t)+D_pu(t) \tag{28}$$

where

$$\hat{A}_p=\left(\hat{S}_{11}+\hat{S}_{12}\hat{M}\hat{S}_{21}\right)F \tag{29}$$

$$\hat{B}_p=\hat{S}_{13}+\hat{S}_{12}\hat{M}\hat{S}_{23} \tag{30}$$

$$\hat{C}_p=\left(\hat{S}_{31}+\hat{S}_{32}\hat{M}\hat{S}_{21}\right)F \tag{31}$$

being

$$\hat{M}=L\left(I-\hat{S}_{22}L\right)^{-1} \tag{32}$$

Next section proposes a two windings transformer including the linear and nonlinear core in the physical domain. Also, a nonlinear of the observer is designed.

V. Bond Graph of a Two Windings Transformer with Core

Charles P. Steinmetz (1865-1923) developed the circuit model that is universally used for the analysis of iron core transformers at power frequencies [1]. However it is good idea to consider transformers first from the point of view of basic linear circuit theory to better appreciate the Steinmetz model.

Consider the magnetic coupling between the primary and secondary windings of a transformer shown in Fig. 3 [12].

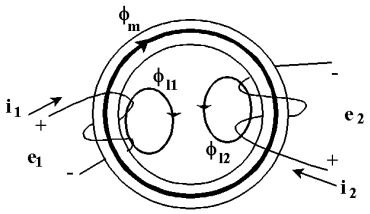

Fig. 3 Magnetic coupling of a two-winding transformer

The total flux linked by each winding may be divided into two components: a mutual component, ϕ_m, that is common to both windings, and a leakage flux components that links only the winding itself. In terms of these flux components, the total flux by each of the windings can be expressed as, $\phi_1=\phi_{l1}+\phi_m$ and $\phi_2=\phi_{l2}+\phi_m$ where ϕ_{l1} and ϕ_{l2} are the leakage flux components of windings 1 and 2, respectively. Assuming that

N_1 turns of winding 1 effectively link ϕ_m and ϕ_{l1}, the flux linkage of winding 1 is defined by, $\lambda_1 = N_1\phi_1 = N_1(\phi_{l1} + \phi_m)$ the leakage and mutual fluxes can be expressed in terms of the winding currents using the magneto-motive forces (mmfs) and permeances. So, the flux linkage of winding 1 is, $\lambda_1 = N_1\left[N_1 i_1 P_{l1} + (N_1 i_1 + N_2 i_2)P_m\right]$ where $P_{l1} = \frac{\phi_{l1}}{N_1 i_1}$ and $P_m = \frac{\phi_m}{N_1 i_1 + N_2 i_2}$.

Similarly, the flux linkage of winding 2 can be expressed as, $\lambda_2 = N_2(\phi_{l2} + \varphi_m)$ and using mmfs and permeances for this winding, $\lambda_2 = N_2\left[N_2 i_2 P_{l2} + (N_1 i_1 + N_2 i_2)P_m\right]$. The resulting flux linkage equations for the two magnetically coupled windings, expressed in terms of the winding inductances are,

$$\begin{bmatrix}\lambda_1\\ \lambda_2\end{bmatrix} = \begin{bmatrix}L_{11} & L_{12}\\ L_{21} & L_{22}\end{bmatrix}\begin{bmatrix}i_1\\ i_2\end{bmatrix} \tag{33}$$

where L_{11} and L_{22} are the self-inductances of the windings, and L_{12} and L_{21} are the mutual inductances between them.

Note that the self-inductance of the primary can be divided into two components, the primary leakage inductance, L_{l1} and the primary magnetizing inductance, L_{m1}, which are defined by, $L_{11} = L_{l1} + L_{m1}$ where $L_{l1} = N_1^2 P_{l1}$ and $L_{m1} = N_1^2 i_1 P_m$.

Likewise, for winding 2 $L_{22} = L_{l2} + L_{m2}$ where $L_{l2} = N_2^2 P_{l2}$ and $L_{m2} = N_2^2 i_2 P_m$.

Finally, the mutual inductance is given by, $L_{12} = N_1 N_2 i_2 P_m$ and $L_{21} = N_1 N_2 i_1 P_m$, taking the ratio of L_{m2} a L_{m1}, then $L_{m2} = \left(\frac{N_2}{N_1}\right)^2 L_{m1}$.

The induced voltage in winding 1 is given by, $e_1 = \frac{d\lambda_1}{dt} = L_{11}\frac{di_1}{dt} + L_{12}\frac{di_2}{dt}$ replacing L_{11} by $L_{l1} + L_{m1}$ and $L_{l2}i_2$ by $N_2 L_{m1} i_2 / N_1$, we obtain $e_1 = L_{l1}\frac{di_1}{dt} + L_{m1}\frac{d\left(i_1 + (N_2/N_1)i_2\right)}{dt}$.

Similarly, the induced voltage of winding 2 is written by, $e_2 = L_{l2}\frac{di_2}{dt} + L_{m2}\frac{d\left(i_2 + (N_1/N_2)i_1\right)}{dt}$.

Finally, the terminal voltage of a winding is the sum of the induced voltage and the resistive drop in the winding, the complete equations of the two windings are,

$$\begin{bmatrix}v_1\\ v_2\end{bmatrix} = \begin{bmatrix}r_1 i_1\\ r_2 i_2\end{bmatrix} + \begin{bmatrix}L_{l1} + L_{m1} & a^{-1}L_{m1}\\ aL_{m2} & L_{l2} + L_{m2}\end{bmatrix}\begin{bmatrix}\frac{di_1}{dt}\\ \frac{di_2}{dt}\end{bmatrix} \tag{34}$$

where $a = N_1 / N_2$.

The final concept involved in the Steinmetz transformer model is a scheme for handling the nonlinearity of the core and the core losses. The Steinmetz model approaches the problem of representing core excitation by first dividing it into two parts: magnetization and core losses [1]. In order to consider the core losses of a transformer a bond graph model is presented in Fig. 4.

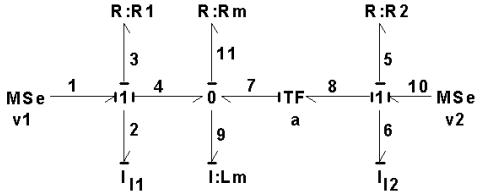

Fig. 4 Bond graph of a complete transformer

The key vectors of the bond graph of Fig. 4 are,

$$x = \begin{bmatrix}p_2\\ p_6\\ p_9\end{bmatrix}; \dot{x} = \begin{bmatrix}e_2\\ e_6\\ e_9\end{bmatrix}; z = \begin{bmatrix}f_2\\ f_6\\ f_9\end{bmatrix} \tag{35}$$

$$D_{in} = \begin{bmatrix}f_3\\ f_5\\ f_{11}\end{bmatrix}; D_{out} = \begin{bmatrix}e_3\\ e_5\\ e_{11}\end{bmatrix}; u = \begin{bmatrix}e_1\\ e_{10}\end{bmatrix}$$

the constitutive relations of the fields are,

$$L = diag\{R_1, R_2, R_m\} \tag{36}$$

$$F = diag\left\{\frac{1}{L_{l1}}, \frac{1}{L_{l2}}, \frac{1}{L_m}\right\} \tag{37}$$

and the junction structure is given by

$$S_{12} = -S_{21}^T = \begin{bmatrix}-1 & 0 & -1\\ 0 & -1 & \frac{-1}{a}\\ 0 & 0 & 1\end{bmatrix}; S_{13} = \begin{bmatrix}1 & 0\\ 0 & 1\\ 0 & 0\end{bmatrix} \tag{38}$$

$$S_{11} = S_{22} = S_{23} = 0$$

By substituting (36), (37) and (38) into (6) and (7), the state space representation of the transformer is,

$$\hat{A}_p = \begin{bmatrix}\frac{-(R_1 + R_m)}{L_{l1}} & \frac{-R_m}{aL_{l1}} & \frac{R_m}{L_{l1}}\\ \frac{-R_m}{aL_{l2}} & \frac{-\left(R_1 + \frac{R_m}{a^2}\right)}{L_{l2}} & \frac{-R_m}{aL_{l2}}\\ \frac{R_m}{L_m} & \frac{-R_m}{aL_m} & \frac{-R_m}{L_m}\end{bmatrix} \tag{39}$$

$$\hat{B}_p = \begin{bmatrix}\frac{1}{L_{l1}} & 0 & 0\\ 0 & \frac{1}{L_{l2}} & 0\end{bmatrix}^T$$

The incorporation of nonlinear effects such as magnetic saturation and hysteresis is achieved in the transformer model with the appropriate modification of the inductance L_m in the bond graph of Fig. 4.

In Fig. 5 the saturation curve is illustrated and this curve is approximated with the equation [15],

$$i_{L_m} = \frac{1}{\beta}\tan\left(\frac{\lambda L_m}{\alpha}\right) \tag{40}$$

where $\alpha = 0.3215$ and $\beta = 0.8642$.

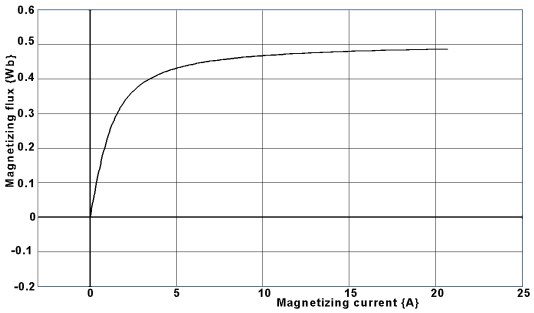

Fig. 5 Saturation curve of equation (40)

In other wise the magnetization inductance of the transformer is defined by

$$L_m = \frac{d\lambda_m}{di_m} = \frac{\alpha\beta}{1+\beta^2 i_m^2} \tag{41}$$

and substituting into (39) we have

$$\dot{z}(t) = \breve{A}z(t) + \overline{B_p}u(t) + G\gamma\left(Hz(t)\right) \tag{42}$$

where

$$\breve{A} = \begin{bmatrix} \frac{-(R_1+R_m)}{aL_{l2}} & \frac{-R_m}{aL_{l1}} & \frac{R_m}{L_{l1}} \\ \frac{-R_m}{aL_{l2}} & \frac{-(R_2+R_m/a^2)}{aL_{l2}} & \frac{R_m}{aL_{l2}} \\ \frac{R_m}{\alpha\beta} & \frac{R_m}{\alpha\beta a} & \frac{-R_m}{\alpha\beta} \end{bmatrix} \tag{43}$$

$$G\gamma(Hz) = \frac{\beta R_m}{\alpha}\left(z_1 z_3^2 + \frac{1}{a} z_2 z_3^2 - z_3^3\right) \tag{44}$$

also

$$G = \begin{bmatrix} 0 & 0 & \frac{\beta R_m}{\alpha} \end{bmatrix}^T \tag{45}$$

$$\gamma(\upsilon) = z_1 z_3^2 + \frac{1}{a} z_2 z_3^2 - z_3^3 \tag{46}$$

and

$$\upsilon = Hz = \begin{bmatrix} 1 & \frac{1}{a} & -1 \end{bmatrix} \begin{bmatrix} z_1 \\ z_2 \\ z_3 \end{bmatrix} \tag{47}$$

therefore

$$\frac{\partial\gamma}{\partial\upsilon} + \left(\frac{\partial\gamma}{\partial\upsilon}\right)^T = 2z_3^2 \geq 0 \forall \upsilon \in \Re \tag{48}$$

The numerical values of the parameters of the bond graph of Fig. 4 are $L_{l1} = 11.05mH$, $L_{l2} = 11.05mH$, $\alpha = 0.3215$; $\beta = 0.8642$; $R_1 = 5.8\Omega$, $R_2 = 5.8\Omega$, $R_L = 100\Omega$, $a = 10$, $R_m = 4K\Omega$ and $\upsilon_1 = 120\sin(377t)$. If we introduce (40) to the bond graph model of Fig. 4, the nonlinear phenomena is incorporated. Fig. 6 shows the saturation performance in the bond graph model of the transformer.

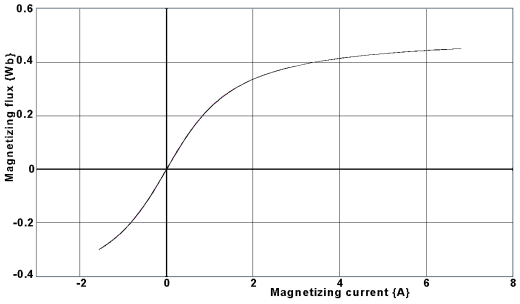

Fig. 6 Nonlinear performance of the transformer of Fig. 4

The primary and secondary current of the bond graph model of the transformer are shown in Fig. 7. Note that the saturation and hysteresis affects both electrical currents on the electrical transformer.

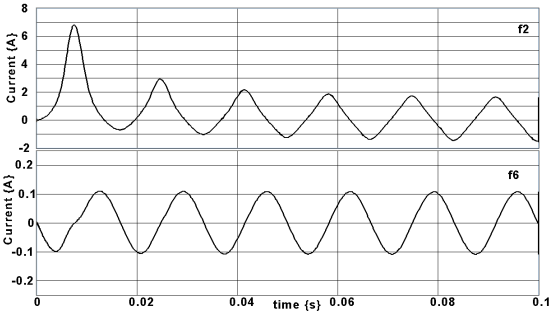

Fig. 7 Primary and secondary current of a transformer with nonlinear core

The observer design using bond graph allows to know the relation between the plant and the observer in an easy way. From (48) the monotonicity property of the electrical transformer is satisfied. Hence, a nonlinear observer for the transformer can be applied. Fig. 8 shows the modeling in bond graph of the nonlinear observer.

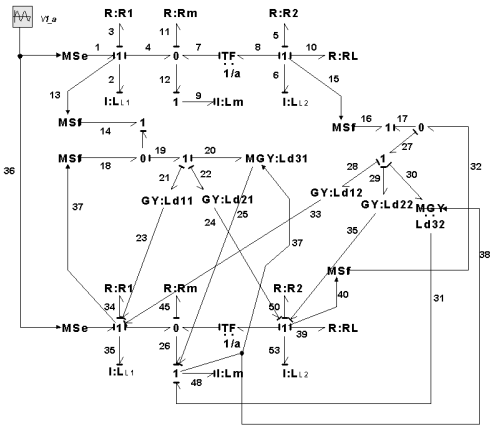

Fig. 8 Observer for the transformer in the physical domain

The nonlinear section for the observer on the bond graph by using modulated gyrators $MGY:Ld_{31}$ and $MGY:Ld_{32}$ with active bonds 37 and 38 is introduced.

In order to prove that the complete bond graph of Fig. 8 represents a system with multivariable monotone

nonlinearities, the mathematical model is obtained. Thus, the key vectors for the transformer is given by (35) and for the observer are,

$$\hat{x}=\begin{bmatrix} p_{35} \\ p_{53} \\ p_{48} \end{bmatrix}; \dot{\hat{x}}=\begin{bmatrix} e_{35} \\ e_{53} \\ e_{48} \end{bmatrix}; \hat{z}=\begin{bmatrix} f_{35} \\ f_{53} \\ f_{48} \end{bmatrix}$$
$$\hat{D}_{in}=\begin{bmatrix} f_{34} \\ f_{50} \\ f_{45} \\ f_{39} \end{bmatrix}; \hat{D}_{out}=\begin{bmatrix} e_{34} \\ e_{50} \\ e_{45} \\ e_{39} \end{bmatrix}; \quad y=\begin{bmatrix} f_2 \\ f_6 \end{bmatrix}; \quad \hat{y}=\begin{bmatrix} f_{35} \\ f_{53} \end{bmatrix} \tag{49}$$

the constitutive relations of the elements are,

$$F=diag\left\{\frac{1}{L_{l1}},\frac{1}{L_{l2}},\frac{1}{L_m}\right\} \tag{50}$$

$$L=diag\{R_1,R_2,R_m,R_L\} \tag{51}$$

and the junction structure is

$$\hat{S}_{11}=\begin{bmatrix} Ld_{11} & Ld_{12} & 0 \\ Ld_{21} & Ld_{22} & 0 \\ Ld_{31} & Ld_{32} & 0 \end{bmatrix}; \hat{S}_{13}=\begin{bmatrix} 1 & 0 \\ 0 & 1 \\ 0 & 0 \end{bmatrix}$$
$$S_{12}=\begin{bmatrix} -1 & 0 & -1 & 0 \\ 0 & -1 & -a^{-1} & -1 \\ 0 & 0 & 1 & 0 \end{bmatrix}; \hat{S}_{31}=\begin{bmatrix} 1 & 0 & 0 \\ 0 & 1 & 0 \end{bmatrix} \tag{52}$$
$$\hat{S}_{22}=\hat{S}_{23}=\hat{S}_{32}=\hat{S}_{33}=0$$

From (29), (30), (50), (51) and (52) the state space representation is,

$$\widehat{A_p}=\begin{bmatrix} \frac{-R_{11}}{L_{l1}}+G_{11} & \frac{-a^{-1}R_m}{L_{l1}}+G_{12} & \frac{R_m}{L_{l1}} \\ \frac{-a^{-1}R_m}{L_{l2}}+G_{21} & \frac{-R_{22}}{L_{l2}}+G_{22} & \frac{-a^{-1}R_m}{L_{l2}} \\ \frac{R_m}{L_m}+\frac{L_{p31}}{L_m} & \frac{-a^{-1}R_m}{L_m}+\frac{L_{p32}}{L_m} & \frac{-R_m}{L_m} \end{bmatrix} \tag{53}$$
$$B_p=\begin{bmatrix} 1 & 0 \\ 0 & 1 \\ 0 & 0 \end{bmatrix}; \tilde{A}_p=\begin{bmatrix} -G_{11} & -G_{12} & 0 \\ -G_{21} & -G_{22} & 0 \\ \frac{-L_{p31}}{L_m} & \frac{-L_{p32}}{L_m} & 0 \end{bmatrix}$$

where $R_{11}=R_1+R_m$; $R_{22}=R_2+R_L+R_m$; $G_{11}=Ld_{11}/L_{l1}$; $G_{l2}=Ld_{12}/L_{l1}$; $G_{21}=Ld_{21}/L_{l2}$; $G_{22}=Ld_{22}/L_{l2}$; $Lp_{31}=(Ld_{31}+K_{d1}L_m)$; $L_{p32}=(L_{d32}+K_{d2}L_m)$.

In order to verify that (53) is the same observer respect (42). By substituting (41) into the third line of $\hat{A}_p$ from (53) we have,

$$\dot{\hat{z}}_3=\frac{R_m}{\alpha\beta}\left(\hat{z}_1+a^{-1}\hat{z}_2-\hat{z}_3\right)+\frac{\beta R_m}{\alpha}\left(\hat{z}_1+a^{-1}\hat{z}_2-\hat{z}_3\right)\hat{z}_3^2+G \tag{54}$$

where

$$G=\left(Ld_{31}+K_{d1}L_m\right)\frac{\left(\hat{z}_1-z_1\right)}{L_m}+\left(Ld_{32}+K_{d2}L_m\right)\frac{\left(\hat{z}_2-z_2\right)}{L_m} \tag{55}$$

and using one more time (41) into (55) we obtain,

$$G=K_1\left(\hat{z}_1-z_1\right)+\frac{\beta}{\alpha}L_{d31}\left(\hat{z}_1-z_1\right)\hat{z}_3^2+ K_2\left(\hat{z}_2-z_2\right)+\frac{\beta}{\alpha}L_{d32}\left(\hat{z}_2-z_2\right)\hat{z}_3^2 \tag{56}$$

Finally, from (18) the original observer gains are

$$L=\begin{bmatrix} L_{11} & L_{12} \\ L_{21} & L_{22} \\ L_{31} & L_{32} \end{bmatrix}; K=\begin{bmatrix} K_1 & K_2 \end{bmatrix} \tag{57}$$

Therefore, the relations between the graphical gains in bond graph and the original gains for the observer are: $L_{d11}=L_{11}\bullet L_{l1}$; $L_{d12}=L_{12}\bullet L_{l1}$; $L_{d21}=L_{21}\bullet L_{l2}$; $L_{d22}=L_{22}\bullet L_{l2}$; $L_{d31}=\frac{\alpha}{\beta}L_{31}$; $L_{d32}=\frac{\alpha}{\beta}L_{32}$; $K_{d1}=K_1-\frac{L_{31}}{\beta^2}$ and $K_{d2}=K_2-\frac{L_{32}}{\beta^2}$.

By substituting the values of the parameters of the complete system according with (17), we have,

$$A=\begin{bmatrix} -362515.83 & -3619909.50 & 361990.95 \\ -3619909.50 & -36208669.68 & 3619909.50 \\ 14396.75 & 143967.59 & -14396.75 \end{bmatrix}$$
$$B=\begin{bmatrix} 90.49 & 0 \\ 0 & 0 \\ 0 & 0 \end{bmatrix}; C=\begin{bmatrix} 1 & 0 & 0 \\ 0 & 1 & 0 \end{bmatrix}$$
$$H=\begin{bmatrix} 1 & 0.1 & -1 \end{bmatrix}; G=\begin{bmatrix} 0 & 0 & 10752.09 \end{bmatrix}^T$$

The linear matrix inequality LMI must be feasible (25), which guarantees a strict positive real (SPR) property for the linear part of the observer error system, for this system, we obtain

$$P=\begin{bmatrix} 404427 & -404427 & -0.000566 \\ -404427 & 404427 & -0.000836 \\ -0.000566 & -0.000836 & 0.000093 \end{bmatrix}$$
$$L=\begin{bmatrix} -104334.8 & -1035963.5 \\ -104334.8 & -1035963.5 \\ -2306330.8 & -22903046.7 \end{bmatrix}; K=\begin{bmatrix} 5.09 \\ 0.79 \end{bmatrix}^T$$

with $\upsilon=100$.

The performance of the electrical transformer with the observer is shown in Fig. 9 and 10. Fig. 9 illustrates the primary current on the transformer, f_2 and on the observer, f_{35}.

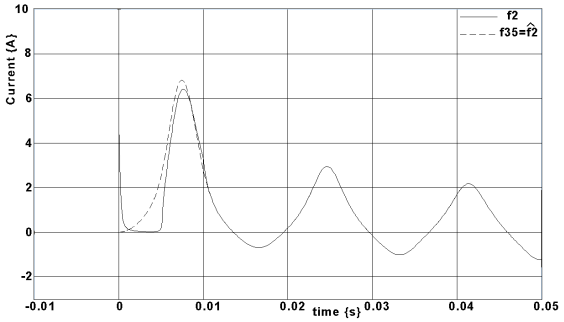

Fig. 9 Primary currents on the transformer and on the observer

The secondary currents on the transformer, f_6 and on the observer, f_{53} are shown in Fig. 10.

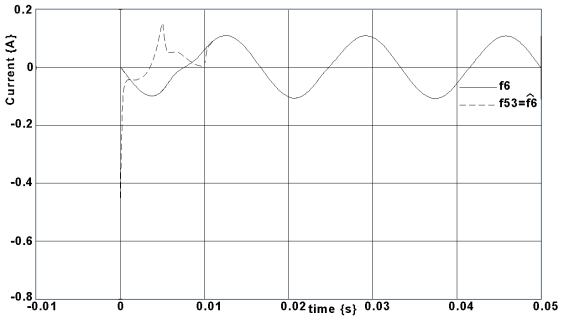

Fig. 10 Secondary currents on the transformer and on the observer

Therefore, the convergency of the estimates respect the true states of the electrical transformer including nonlinear saturation and hysteresis is guaranteed.

VI. Bond Graph of a DC Motor

Of all electric machines the direct (DC) machine is perhaps the most straightforward to analyze. Although a rigorous deviation of the voltage and torque equation is possible it is rather lengthy and little is gained since these relationships may be deduced. The armature coils revolve in a magnetic field established by current flowing in the field winding, which is shown in Fig. 11. We know that voltage is induced in these coils by virtue of this rotation and we can write the field and armature voltage equations as $v_f = r_f i_f + L_f \frac{di_f}{dt}$ and $v_a = wL_a i_f + r_a i_a L_a \frac{di_a}{dt}$ where L_f and L_a are the self inductances of the field and armature windings, respectively. The rotor speed is denoted as w and L_{af} is the mutual inductance between the field and the rotating armature coils.

The expression for torque is $T_e = L_{af} i_f i_a$ and the torque and rotor speed are related by $T_e = J\frac{dw}{dt} + fw + T_L$ where J is the inertia of the rotor and in some cases the connected mechanical load, the constant f is a damping coefficient associated with the mechanical rotational system of the machine and mechanical load.

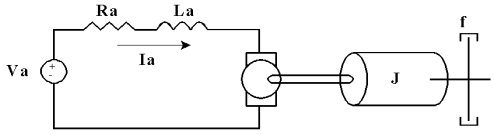

Fig. 11 Scheme of a DC motor with an independent excitation

The bond graph of the DC motor is shown in Fig. 12.

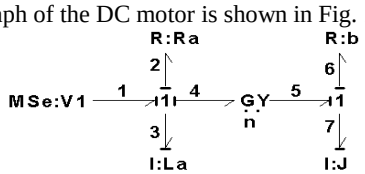

Fig. 12 Bond graph of the DC motor

The key vectors of the bond graph are

$$x = \begin{bmatrix} p_3 \\ p_7 \end{bmatrix}; \dot{x} = \begin{bmatrix} e_3 \\ e_7 \end{bmatrix}; z = \begin{bmatrix} f_3 \\ f_7 \end{bmatrix}; D_{in} = \begin{bmatrix} f_2 \\ f_6 \end{bmatrix}; D_{out} = \begin{bmatrix} e_2 \\ e_6 \end{bmatrix}; \begin{matrix} u = e_1 \\ y = f_7 \end{matrix}$$

the constitutive relations are

$$F = diag\left\{\frac{1}{L_a}, \frac{1}{J}\right\} \tag{58}$$

$$L = diag\{R_a, b\} \tag{59}$$

and the junction structure is

$$\begin{aligned} S_{11} &= \begin{bmatrix} 0 & -n \\ n & 0 \end{bmatrix}; S_{13} = \begin{bmatrix} 1 \\ 0 \end{bmatrix} \\ S_{12} &= -S_{21}^T = -I; S_{31} = \begin{bmatrix} 0 & 1 \end{bmatrix} \\ S_{22} &= S_{23} = S_{32} = S_{33} = 0 \end{aligned} \tag{60}$$

The state equation of the DC motor is

$$A_p = \begin{bmatrix} \frac{-R_a}{L_a} & \frac{-n}{J} \\ \frac{n}{L_a} & \frac{-b}{J} \end{bmatrix}; B_p = \begin{bmatrix} 1 \\ 0 \end{bmatrix}; C_p = \begin{bmatrix} 0 & \frac{1}{J} \end{bmatrix}; D_p = 0$$

Now, if we consider a magnetic saturation of the inductance, L_a, according to the model given in (40), the state equation with saturation is

$$\overline{A_p} = \begin{bmatrix} \frac{-R_a}{\alpha\beta} & \frac{-n}{J} \\ \frac{n}{\alpha\beta} & \frac{-b}{J} \end{bmatrix}; G\gamma(Hz) = \begin{bmatrix} \frac{-R_a\beta}{\alpha} x_1^3 \\ \frac{\beta}{\alpha} x_1^3 \end{bmatrix}$$

the vector $G\gamma(Hx)$ can be decomposed as

$$G\gamma(Hx) = \begin{bmatrix} \frac{-1}{3} & 0 \\ 0 & \frac{-1}{3} \end{bmatrix} \begin{bmatrix} 3R_a\beta x_1^2 & 0 \\ -3\beta x_1^2 & 0 \end{bmatrix} \begin{bmatrix} 1 & 0 \\ 0 & 1 \end{bmatrix} \begin{bmatrix} x_1 \\ x_2 \end{bmatrix}$$

then $\gamma(\upsilon) = \begin{bmatrix} \frac{3R_a\beta}{\alpha} x_1^3 \\ \frac{-3\beta}{\alpha} x_1^3 \end{bmatrix}$ and $\upsilon = Hx = \begin{bmatrix} 1 & 0 \\ 0 & 1 \end{bmatrix} \begin{bmatrix} x_1 \\ x_2 \end{bmatrix}$

the monotonicity property applied to this example, gives,

$$\frac{\partial \upsilon(x_1, x_2)}{\partial (x_1, x_2)} = \begin{bmatrix} 0 \\ 0 \end{bmatrix}$$

then (16) is satisfied.

Thus, an nonlinear observer is designed and is shown in Fig. 13.

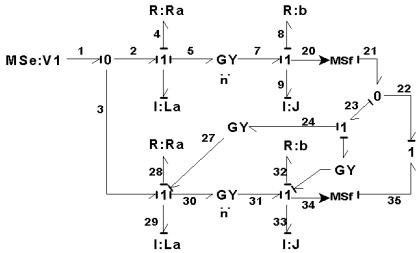

Fig. 13 Observer of the DC motor

The key vectos for the observer are,

$$\dot{\hat{x}} = \begin{bmatrix} p_{29} \\ p_{33} \end{bmatrix}; \hat{x} = \begin{bmatrix} e_{29} \\ e_{33} \end{bmatrix}; \hat{z} = \begin{bmatrix} f_{29} \\ f_{33} \end{bmatrix}; \hat{D}_{in} = \begin{bmatrix} f_{28} \\ f_{32} \end{bmatrix}; \hat{D}_{out} = \begin{bmatrix} e_{28} \\ e_{32} \end{bmatrix}; \; u = e_1 \; y = f_{34}$$

the junction structure for the observer is

$$\hat{S}_{11} = \begin{bmatrix} 0 & -n - L_1 \\ n & L_2 \end{bmatrix}; \tilde{S} = \begin{bmatrix} 0 & L_1 \\ 0 & -L_2 \end{bmatrix}; \hat{S}_{13} = \begin{bmatrix} 1 \\ 0 \end{bmatrix} \qquad (61)$$

$$\hat{S}_{21} = -\hat{S}_{12}^T = I_2; \hat{S}_{22} = \hat{S}_{23} = 0$$

From (27), (29), (30), (58), (59) and (61), the observer state equation is

$$\dot{\hat{x}} = \begin{bmatrix} \frac{-R_a}{L_a} & -\frac{n+L_1}{J} \\ \frac{n}{L_a} & \frac{L_2 - f}{J} \end{bmatrix} \hat{x} + \begin{bmatrix} 0 & \frac{L_1}{J} \\ 0 & \frac{L_2}{J} \end{bmatrix} x + \begin{bmatrix} 1 \\ 0 \end{bmatrix} e_1$$

if we consider the magnetic saturation given by (41) then

$$\dot{\hat{x}}_1 = \frac{-R_a}{\alpha\beta}\hat{x}_1 - \frac{n}{J}\hat{x}_2 + \frac{L_1}{J}(\hat{x}_2 - x_2) + \frac{R_a\beta}{\alpha}x_1^2\left(\hat{x}_1 + \frac{k_1}{J}(\hat{x}_2 - x_2)\right) + u$$

and $\dot{\hat{x}}_2 = \frac{n}{\alpha\beta}\hat{x}_1 - \frac{f}{J}\hat{x}_2 + \frac{L_2}{J}(\hat{x}_2 - x_2) - \frac{\beta}{\alpha}x_1^2\left(\hat{x}_2 + \frac{k_1}{J}(\hat{x}_2 - x_2)\right)$

The numerical parameters of the DC motor are: $e_1 = 10$, $n = 3$, $R_a = 0.5$, $f = 1.5$, $\alpha = 1$, $\beta = 1$, $J = 1.5$, $H = I_2$, $G = \frac{-1}{3}I_2$, $P = diag\{0.56, 0.33\}$, $L = [1 \;\; 1]^T$; $k = [0 \;\; -1.33]^T$.

Hence, simulation results of each state variable are shown in Fig. 14 and 15.

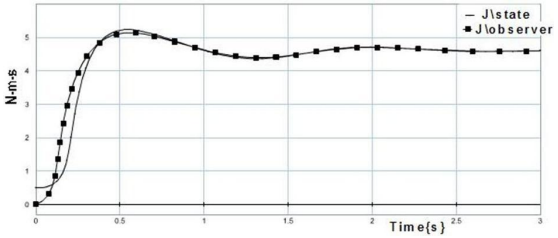

Fig. 14 State and observer of x_1

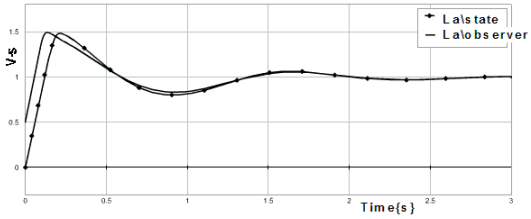

Fig. 15 State and observer of x_2

VII. Conclusions

A bond graph approach to design observers with multivariable nonlinearities is proposed. Hence, models of a power transformer and a DC motor incorporating the nonlinear saturation in the physical domain is presented. In order to prove the results, the graphical simulations are shown. The convergence of the estimates and the states of the transformer by using simulation is described.

References

[1] George McPerson and Robert D. Laramore, *An Introduction to Electrical Machines and Transformers*, John, Wiley & Sons, 1990.

[2] Dean C. Karnopp, Donald L. Margolis and Ronald C. Rosenberg, *System Dynamics Modeling and Simulation of Mechatronic Systems*, Wiley, John & Sons, 2000.

[3] P. E. Wellstead, *Physical System Modelling*, Academic Press, London, 1979.

[4] C. Pichardo-Almarza, A. Rahmani, G. Dauphin-Tanguy, M. Delgado, "High gain observers for non-linear systems modelled by bond graphs", *Proc. IMechE Part I: J. Systems and Control Engineering*, 219(2005) pp. 477-497.

[5] Gilberto Gonzalez-A, R. Galindo, "Direct Control in Bond Graph by State Estimated Feedback for MIMO LTI Estimated", *Proceedings of the 2002 IEEE International Conference on Control Applications*, Scotland, pp. 1183-1188.

[6] Cesar Pichardo-Almarza, A. Rahmani, G. Dauphin-Tanguy, M. Delgado, "Using the Bicausality concept to build reduced order observers in linear invariant systems modelled by bond graph", *Mathematical and Computer Modelling of Dynamical Systems*, Vol. 12, issues: 2-3, pp. 219-234, 2006.

[7] Peter J. Gawthrop, "Physical Model-based Control: A Bond Graph Approach", *Journal of the Franklin Institute*, 332B(3), pp. 285-305, 1995.

[8] Rafael Martinez-Guerra, J. De Leon-Morales, "On Nonlinear Observers", *Proceedings of the 1997 IEEE International Conference on Control Applications*, pp. 324-328, 1997.

[9] Xingzhe Fan, M. Arcak, "Observer design for systems with multivariable monotone nonlinearities", *Systems & Control Letters*, 50(2003) pp. 319-330.

[10] Xingzhe Fan, M. Arcak, "Nonlinear Observer Design for Systems with Multivariable Monotone Nonlinearities", *Proceedings of the 41st IEEE Conference on Decision and Control*, pp. 684-688, 2002.

[11] Z. Q. Wu, G. H. Shirkoohi, J. Z. Cao, "Simple dynamic hysteresis modelling of three phase power transformer", *Journal of Magnetism and Magnetic Materials* 160(1996) pp.79-80.

[12] Chee-Mun Ong, *Dynamic Simulation of Electric Machinery Using MatLab/Simulink*, Prentice-Hall, 1998.

[13] H. Fraisse, J. P. Masson, F. Marthouret and H. Morel, "Modeling of a Non-Linear Conductive Magnetic Circuit. Part 2: Bond Graph Formulation", *IEEE Transactions on Magnetics* Vol. 31, No. 6, November 1995.

[14] C. Sueur and G. Dauphin-Tanguy, "Bond graph approach for structural analysis of MIMO linear systems", *Journal of the Franklin Institute*, Vol. 328, No. 1, pp. 55-70, 1991.

[15] S. Garcia, A. Medina and C. Perez, "A state space single-phase transformer model incorporating nonlinear phenomena of magnetic saturation and hysteresis for transient and period steady-state analysis", *IEEE Power Engineering Society Summer Meeting*, Vol. 4, pp. 2417-2421, July 2000.

[16] M. Arcak, P. Kokotovic, Nonlinear observers: a circle criterion design and robustness, *Automatica* 37(12) (2001) 1923-1930.